

Article

Smart Nanocarrier Based on Poly(oligo(ethylene glycol) methyl ether acrylate) Terminated pH-Responsive Polymer Brushes Grafted Mesoporous Silica Nanoparticles

Amal Alfawaz ^{1,†}, Khalid Alzahrani ^{2,3,†}, Abdurahman Niazy ⁴, Hamdan Alghamadi ⁵, Rhodanne Lambarte ⁶, Abeer Beagan ¹, Latifah Alfahid ⁷, Khalid Alotaibi ^{1,3,*}, and Abdullah Alswieleh ^{1,*}

- ¹ Department of Chemistry, College of Science, King Saud University, Riyadh 11451, Saudi Arabia; amalf@ksu.edu.sa (A.A.); abeagan@ksu.edu.sa (A.B.)
- ² Department of Physics and Astronomy, College of Science, King Saud University, Riyadh 11451, Saudi Arabia; alzkhalid@ksu.edu.sa
- ³ King Abdullah Institute for Nanotechnology, King Saud University, Riyadh 11451, Saudi Arabia
- ⁴ Department of Oral Medicine and Diagnostic Sciences, College of Dentistry, King Saud University, Riyadh 11451, Saudi Arabia; aaniazy@ksu.edu.sa
- ⁵ Department of Periodontics and Community Dentistry, College of Dentistry, King Saud University, Riyadh 11451, Saudi Arabia; dalghamdi@ksu.edu.sa
- ⁶ Molecular and Cell Biology Laboratory, Prince Naif bin AbdulAziz Health Research Center, College of Dentistry, King Saud University, Riyadh 11451, Saudi Arabia; rlambarte@ksu.edu.sa
- ⁷ Department of Physics, College of Science, University of Ha'il, Ha'il 2240, Saudi Arabia; l.alfahid@uoh.edu.sa
- * Correspondence: khalid.m@ksu.edu.sa (K.A.); aswieleh@ksu.edu.sa (A.A.)
- † These authors contributed equally to this work.



Citation: Alfawaz, A.; Alzahrani, K.; Niazy, A.; Alghamadi, H.; Lambarte, R.; Beagan, A.; Alfahid, L.; Alotaibi, K.; Alswieleh, A. Smart Nanocarrier Based on Poly(oligo(ethylene glycol) methyl ether acrylate) Terminated pH-Responsive Polymer Brushes Grafted Mesoporous Silica Nanoparticles. *Appl. Sci.* **2022**, *12*, 3688. <https://doi.org/10.3390/app12073688>

Academic Editors: Ana Paula Betencourt Martins Amaro and Andrea Dorigato

Received: 23 February 2022

Accepted: 30 March 2022

Published: 6 April 2022

Publisher's Note: MDPI stays neutral with regard to jurisdictional claims in published maps and institutional affiliations.



Copyright: © 2022 by the authors. Licensee MDPI, Basel, Switzerland. This article is an open access article distributed under the terms and conditions of the Creative Commons Attribution (CC BY) license (<https://creativecommons.org/licenses/by/4.0/>).

Abstract: A platform technology based on inorganic/organic nanoparticles for carrying drugs could be of enormous potential benefit in treating cancer. Surface modification of the nanoparticles with pH-responsive and biocompatible polymers can improve the selectivity and targeting toward the tumor cells. Polyethylene glycol (PEG) and its derivatives being present on the surface could enhance the ability to tailor nanomaterial hydrophilicity and to resist the adhesion of proteins and/or cells. Herein, we report a new nanoplatform based on mesoporous silica nanoparticles (MSNs) conjugated with poly(2-(diethylamino) ethyl methacrylate) (PDEAEMA) brushes as a candidate for stimuli-responsive intracellular drug delivery system. Alkyl bromide functional initiators (end-functionalized PDEAEMA brushes) were derivatized to amine, followed by the reaction with ethylene sulfide and poly(oligo(ethylene glycol) methyl ether acrylate) (POEGMEA). Using X-ray photoelectron spectroscopy (XPS) to examine the attachment of POEGMEA, it was found that the POEGMEA molecules in the outer surface of PDEAEMA brushes have been successfully reacted with thiol groups, as indicated by the increase in the peak intensity of the C–O group at 286.5 eV. Brush-modified silica hybrids have an average diameter of ca. 250 nm, as estimated by scanning electron microscopy (SEM) and transmission electron microscopy (TEM). Rhodamine B dye was loaded into the brush-modified silica hybrids nanoparticles with loading capacity of ca. 74%. The accumulated dye released from brush-modified particles in acidic media was approximately 60%, whereas the dye amount release in basic media was less than 15% after 10 h exposure time. Alamar Blue assay was used to assess the cytotoxicity of MSNs–PDEAEMA, MSNs–PDEAEMA–SH, and MSNs–PDEAEMA–POEGMEA. The results show that all three nanosystems were non-toxic to hMSC with an increase in cell proliferation for MSNs–PDEAEMA–POEGMEA at 50 µg/mL after both 24 and 48 h of incubation.

Keywords: mesoporous silica nanoparticles; polymer brushes; surface modification; drug delivery; biocompatible nanosystem

1. Introduction

Worldwide, cancer is the second leading cause of death at ages under 70. As estimated, 10 million cancer deaths and 19.3 million new cancer cases occurred in 2020 [1]. Cancer cells can easily proliferate indefinitely and quickly relocate to normal and intact tissues. The cancerous tissues have an excessive metabolite accumulation of the biological microenvironment, leading to increased acidity and hypoxia [2,3]. Treating cancer cells could be achieved using stimuli-sensitive drug delivery systems (DDSs), which are designed to selectively release drug molecules inside the targeted microenvironment of diseased tissues to improve anti-cancer activity [4,5]. The penetration of the drug-loaded nanocarriers into the desired sites of tumour cells rely upon different factors such as cellular internalization, tumour tissue penetration, and prolonged blood circulation [6,7]. Designing an ideal drug delivery system requires the release of the therapeutic agent to the desired site in the right dose within a specified period of time [8].

Mesoporous silica nanoparticles (MSNs) have been suggested to be a good platform for in vivo delivery of anti-cancer drugs to tumour tissues [9–11]. Silica has been considered as a safe material by the Food and Drug Administration (FDA) [12]. MSNs have several characteristics such as stable mesostructure, high surface area and pore volume, uniform pore size, modifiable morphology, and outstanding biocompatibility [13–15]. In the biological environments, unmodified MSNs loaded with anti-cancer drugs are more likely to agglomerate and suffer from lack of specificity [16,17]. These drawbacks have been significantly minimized by the incorporation of biocompatible and stimuli-responsive polymers into the MSNs surface to produce materials with different morphologies such as Yolk-shell and brushes [18,19]. Such polymers allow the host-encapsulated drug molecules to be released in the targeted site in an optimal manner [20–22]. Many biocompatible polymeric shells are considered to be stable in biological environments, which could minimize the side effects and toxicity of DDSs [23,24].

Recently, many studies have been reported on the development of MSN-based pH-responsive systems as a mean of controlling the drug release [25,26]. Polymers that are pH-responsive can undergo reversible and controllable conformational structure changes by changing the pH value of their environments [27]. For illustration, poly(*N,N* diethylaminoethyl methacrylate), poly(*N,N* -dimethylaminoethyl methacrylate), and poly(*b*-amino ester) are base polymers and their amine end-groups experience structural changes when they become protonated. Alswieleh et al. synthesised poly(2-(*tert*-butylamino)ethyl methacrylate) brushes (PTBAEMA) grafted into MSNs using surface-initiated atom transfer radical polymerization (SI-ATRP) techniques. It was found that PTBAEMA brushes became swollen and protonated at a low pH value. In contrast, PTBAEMA brushes became collapsed and deprotonated at a high pH value (>7.5) [28]. Another example of a base polymer is poly(2-(diethylamino)ethyl methacrylate) (PDEAEMA), which can change from hydrophobic to hydrophilic in an acidic medium due to protonation process of tertiary amino groups [29]. Beagan et al. reported the synthesis of hollow mesoporous silica nanoparticles, coated with PDEAEMA brushes terminated with glucosamine [30]. This nanosystem was encapsulated with doxorubicin (DOX), and the results showed that the particle size increased from ca. 500 to ca. 980 nm after decreasing the pH from 9 to 6.5, leading to release DOX-drug within a controlled manner. Alswieleh et al. reported the synthesis of PDEAEMA brushes on mesoporous magnetic nanoparticles and modified them further with folic acid. It was found that ca. 20% and 5% of DOX was released in acidic and basic media, respectively [19].

Poly(ethylene glycol) (PEG) molecules have been attached onto MSNs' surface in order to enhance the water dispersibility of MSNs and also to tailor the hydrophilicity to control protein adhesion [31,32]. A combination of MSNs with mixed-block polymeric micelles composed of poly(ethylene glycol)-block-poly(*l*-lactide) (PEG-PLLA) and poly(ethylene glycol)-block-poly(*d*-lactide) (PEG-PDLA) enhanced the performance of the controlled drug delivery compared to the polymers alone [33]. PEGylation of MSNs' surface increases the diffusion rate of drug molecules into tumor tissues and also improves their colloidal sta-

bility [34]. Alswieleh et al. prepared MSNs coated with a diblock copolymer, consisting of poly(ethylene glycol) methyl ether methacrylate and 2-(tert-butylamino)ethyl methacrylate via the atom transfer radical polymerization method [35]. The results showed that ca. 60% of the loaded DOX-drug was released at $\text{pH} < 6.5$. Alotaibi et al. reported the preparation a pH-responsive nanosystem consisting of PDEAEMA brush grafted on MSNs' surface and modified by cysteine and poly(oligo(ethylene glycol) methyl ether methacrylate) (MSNs-PDEAEMA-Cys-POEGMEMA) and was examined as an anti-cancer drug (DOX) nanocarrier [36]. The DOX was unloaded at basic pH above pH 7 and was successfully released at low pH below 5 due to the protonation process of tertiary amine groups of PDEAEMA. Feng et al. prepared amphiphilic block copolymers made of poly(N,N-diethylaminoethyl methacrylate) and poly(poly(ethylene glycol) methyl ether methacrylate) used to control release of the paclitaxel from MSNs using a pH-trigger. The results showed that about 55% of paclitaxel was released in the intracellular environment at pH 5 [37].

In this current work, we report the synthesis of MSNs with average particle size of 230 nm and average pore size of 5 nm, as estimated by TEM. Surface-initiated activators regenerated by an electron transfer atom transfer radical polymerization (SI-ARGET-ATRP) technique have been used to grow poly(2-(diethylamino) ethyl methacrylate) (PDEAEMA) on the outer surface of MSNs, as pH-sensitive gatekeepers. To enhance the diffusion rate of drug molecules onto tumor tissues and improve their colloidal stability, poly(oligo(ethylene glycol) methyl ether acrylate) (POEGMEA) molecules were then bounded to the outer surface of PDEAEMA brushes via the thiol-Michael addition click reaction. The attachment of POEGMEA was confirmed by XPS and DLS. The synthesized nanosystem was then loaded with Rhodamine B dye (RhB), and the release profile of the dye was investigated in acidic and basic media. The nanocarriers were evaluated for cytotoxic activity against a stem cell line. All nanosystems were found to be nontoxic at concentrations between 10 and 100 $\mu\text{g}/\text{mL}$ for an exposure time of 48 h.

2. Materials and Methods

2.1. Materials

Poly(ethylene glycol) methyl ether acrylate (Methoxy PEG acrylate, POEGMEA, average M_n 480), tetraethyl orthosilicate (TEOS, 98%), hexadecyltrimethylammonium bromide (CTAB, 98%), triphenylphosphine (PPh_3 , 99%), dimethylphenyl phosphine (99%), 2-(diethylamino)ethyl methacrylate (DEAEMA) (99%), copper (II) bromide (CuBr_2 , 98%) 2-bromo-2-methylpropionylbromide (BIBB, 98%), 2,2'-bipyridine (bipy, 99%), ammonium hydroxide aqueous (32 wt%), pyridine (analytical grade), tetrahydrofuran (THF, HPLC grade), ethylene sulfide (98%), ethanol (HPLC grade), (3-aminopropyl) triethoxysilane (APTES, >98%), dimethylformamide (99.9%), methanol (HPLC grade) Rhodamine B, and dichloromethane (DCM, HPLC grade) were purchased from Sigma-Aldrich. Sodium azide (99%) and triethylamine (TEA, 99%) were obtained from Loba Chemie. Ammonium nitrate (NH_4NO_3 , 99%) was purchased from Winlab. L-Ascorbic acid (98%) was purchased from Riedel-de Haën. Deionized water was obtained from an Elga Pure Nanopore system with a resistivity of 15 $\text{M}\Omega\cdot\text{cm}$.

2.2. Preparation Methods

2.2.1. Mesoporous Silica Nanoparticles

To synthesize MSNs, 1.0 g CTAB dissolved in 150 mL deionized water was placed in a 250 mL round-bottom flask. Ammonium hydroxide (32%, 6 mL) was added to form a clear solution. TEOS (5 mL) dissolved in 20 mL hexane was added to the aqueous solution within 30 min under continuous stirring at 200 rpm and 37 °C. The nanoparticles were separated by centrifugation and washed with deionized water and methanol after 12 h.

2.2.2. Mesoporous Silica Nanoparticles Propyl Amine (MSNs-Pr-NH₂)

Amine group modified silica surface was obtained by suspending 1 g of MSNs in a mixture of 0.5 mL APTES and 50 mL toluene. The suspension was heated overnight at 120 °C. The particles were separated by centrifugation and washed with toluene and methanol.

2.2.3. Channel Formation on MSNs-Pr-NH₂

CTAB was extracted by suspending 1 g of MSNs-Pr-NH₂ in 50 mL solution of ammonium nitrate in ethanol (0.13 M). The mixture was heated at 80 °C and allowed to extract for 24 h. The particles were separated by centrifugation and washed with deionized water and methanol.

2.2.4. ATRP Initiator Functionalized Outer Surface of MSNs (MSNs-Br)

ATRP Initiator modified silica surface was obtained by suspending 1 g of MSNs-Pr-NH₂ in a mixture of 0.5 mL TEA and 50 mL DCM. To the mixture, 0.25 mL 2-bromo-2-methylpropionyl bromide was added and allowed to react for 24 h. The particles were separated by centrifugation and washed with DCM and methanol.

2.2.5. Poly(2-(diethylamino) ethyl methacrylate) Brushes Functionalized Outer Surface of MSNs (MSNs-PDEAEMA)

PDEAEMA brushes modified silica surface was obtained by suspending 0.5 g of MSNs-Br in a mixture of 3 mL deionized water and 12 mL ethanol. The mixture was degassed with N₂ for 20 min under stirring. DEAEEMA (2 mL), 0.007 g bipy, and 0.001 g CuBr₂ were added and degassed further for 15 min. Ascorbic acid (0.008 g) was added to the polymerization solution and allowed to react under N₂ for 150 min. The particles were separated by centrifugation and washed with deionized water and methanol.

2.2.6. Amine Groups Modified Surface of Poly(2-(diethylamino) ethyl methacrylate) Brushes Functionalized MSNs (MSNs-PDEAEMA-NH₂)

MSNs-PDEAEMA (0.5 mg) was suspended in 20 mL DMF and degassed with N₂. In a separate flask, 0.15 g of NaN₃ was dissolved in 10 mL degassed DMF, forming a saturated solution of sodium azide. The saturated solution was transferred to the MSN-PDEAEMA mixture under N₂ and heated at 75 °C overnight. The particles were isolated by centrifugation and washed with DMF.

The separated nanoparticles were suspended in 20 mL DMF and degassed with N₂. In a separate flask, 0.5 g of PPh₃ was dissolved in 10 mL degassed DMF, forming a saturated solution of sodium azide. The saturated solution was transferred to the MSN-PDEAEMA mixture under N₂ and heated at 75 °C overnight. The particles were isolated by centrifugation and washed with DMF, deionized water, and methanol.

The solid was suspended in 20 mL mixture of H₂O/THF (1:1), and degassed with N₂ at 50 °C overnight. The particles were separated by centrifugation and washed with DMF, deionized water, and methanol.

2.2.7. Methoxy PEG Acrylate on Outer Surface of MSNs-PDEAEMA (MSNs-PDEAEMA-POEGMEA)

Thiol group modified outer surface of MSNs-PDEAEMA was obtained by suspending 0.5 g of MSNs-PDEAEMA-NH₂ in 30 mL ethanol. To the suspension, 0.3 mL ethylene sulfide was added and stirred overnight at room temperature. The particles were separated by centrifugation and washed with ethanol.

To functionalize the nanoparticles with POEGMEA, 0.5 g of thiol group modified MSNs-PDEAEMA was suspended in a mixture of 1 mL POEGMEA and 30 mL deionized water and stirred at room temperature. Dimethylphenyl phosphine (20 µL) was added to the mixture and stirred at 20 °C overnight. The particles were separated by centrifugation and washed with deionized water and ethanol.

2.3. Measurement and Characterization

The morphology of the nanoparticles was illustrated by scanning electron microscopy (SEM), model JEOL JSM-7610F at 15 kV. The mesostructure of the silica nanoparticles was illustrated by transmission electron microscopy (TEM), model JEOL JEM-1400 at 100 kV. For infrared spectra, the samples were prepared in potassium bromide pellets at the region of 4000–400 cm^{-1} with a resolution of 4 cm^{-1} . Fourier transform infrared (FT-IR) spectrometer was a PerkinElmer Spectrum BX FTIR. High-resolution XPS spectra of the sample was obtained by JEOL JPS-9030 photoelectron spectrometer, employing mg $\text{K}\alpha$ X-rays. Ultraviolet–visible absorption spectra were obtained by a SpectraMax Plus 384 microplate reader.

2.4. The Rate Loading and Release of Rhodamine B (Rh B)

Generally, the nanoparticles (1 mg) were dispersed in 1 mL phosphate-buffered saline (PBS) buffer solution at pH 3. Rh B solution (1 mL, 2 mg/mL) was added to the suspension and left at room temperature overnight at a shaking rate of 150 rpm. The pH value was then adjusted to ~8 using a diluted solution of sodium hydroxide and shaken for another 2 h. The solid was separated, and the concentration of unloaded dye was determined by UV–Vis spectrophotometer at wavelength of 554 nm.

The dye loading capacity (LC) and encapsulation efficiency (EE) were calculated by:

$$\text{LC} = (\text{the amount of total entrapped dye} / \text{the total nanoparticle weight}) \times 100 \quad (1)$$

$$\text{EE} = (\text{entrapped quantity of dye} / \text{total quantity of dye}) \times 100 \quad (2)$$

Dye release experiments were performed by suspending 1 mg of the dye loaded nanosystem into 1 mL PBS at different pHs, at 37 °C under shaking rate 150 rpm. At different times, the solution was separated, and the amount of dye released was determined by UV–Vis spectrophotometer at a wavelength of 554 nm. After each collection, the solution volume was kept constant by addition 1 mL of fresh medium.

2.5. Cell Culturing and Cytotoxicity

Human bone marrow-derived mesenchymal stem cells (hMSCs) were immortalized by the genetic overexpression of telomerase reverse transcriptase (Abdallah et al. 2005). Human MSCs were cultured until confluency in Dulbecco's Modified Eagle's Medium (DMEM) supplemented with 10% fetal bovine serum (FBS), 1% penicillin-streptomycin, and 1% non-essential amino acids (all from Gibco, Invitrogen, USA) at 37 °C and 5% CO_2 . Upon confluency, hMSCs were seeded at a concentration of 10×10^3 cells/well in 96-well plates. Cells were treated with different nanoparticles at concentrations of 10, 50, and 100 $\mu\text{g}/\text{mL}$ for 24 and 48 h.

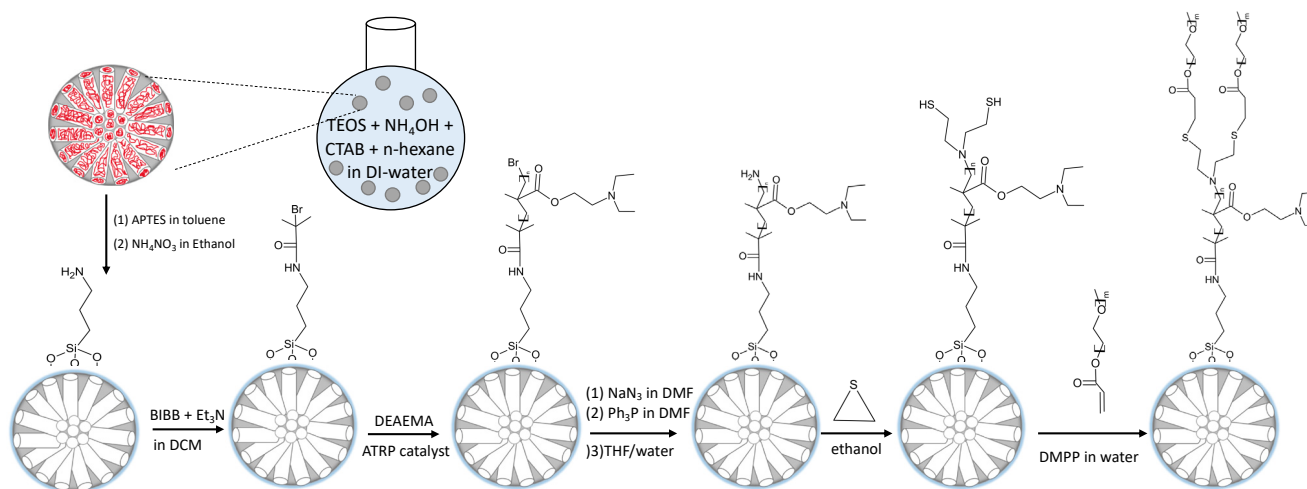
Alamar Blue assay (AbD Serotec, NC, USA) was used to measure cell viability of human mesenchymal stem cells exposed to nanosilica particles according to the manufacturer's instructions. After each incubation time period, 10% (*v/v*) Alamar Blue reagent was added to the treated wells and incubated for 4 h at 37 °C. The fluorescence signal from the samples was measured at an excitation wavelength of 530 nm and an emission wavelength of 590 nm using a BioTek Synergy HT plate reader (Winooski, VT, USA), and the cell proliferation measurement was calculated as follows:

$$\text{Cell proliferation (\%)} = \frac{\text{OD of Control} - \text{OD of treated}}{\text{OD of Control}} \times 100 \quad (3)$$

Results from three independent experiments were obtained. The software used for analysis was GraphPad Prism 6.0 (San Diego, CA, USA).

3. Results and Discussion

The nanoplatform was prepared in multiple steps, as shown in Scheme 1. First, propylamine was anchored to the outer surface of the MSNs, followed by CTAB extraction using ion exchange process via ammonium nitrate in ethanol, to allow guest molecules incubate in the internal pore surface. Amino groups were then reacted with BIBB to initiate the surface. The SI-ARGET-ATRP technique was used to grow PDEAEMA brushes on the MSNs' outer surface, to work as gate keeper for guest molecules. Bromine atom-terminated PDEAEMA chains were substituted to amines, via NaN_3 and PPh_3 . Amine group-terminated PDEAEMA chains were reacted with ethylene sulfide to have thiol groups at the end of polymer chains. POEGMEA was capped onto the outer surface of the nanoparticles via thiol-ene chemistry, thiol-Michael reaction mediated by dimethylphenyl phosphine.



Scheme 1. Schematic illustration of the synthesis route of the mesoporous silica nanoparticles (MSNs) modified with poly(2-(diethylamino) ethyl methacrylate) (PDEAEMA) brushes capped with poly(oligo(ethylene glycol) methyl ether acrylate) (POEGMEA).

FTIR analysis for the prepared samples was performed to confirm the organic molecules attached to the MSNs outer surface (Figure 1). For MSNs IR spectra, wide bands between 1000 and 1250 cm^{-1} were assigned to stretching bands of Si–O–Si, and the band at $\sim 800\text{ cm}^{-1}$ was assigned to the stretching vibration of Si–O. The C–H stretching vibration at $\sim 2900\text{ cm}^{-1}$ disappeared after the extraction process. New peaks were observed at ~ 1450 and $\sim 1380\text{ cm}^{-1}$, corresponding to C–H bending vibration of the methyl group after the initiation step. After the ATRP polymerization process, a new peak was observed at $\sim 1730\text{ cm}^{-1}$ in all polymer-coated MSNs samples, appointed to C=O stretching vibrations.

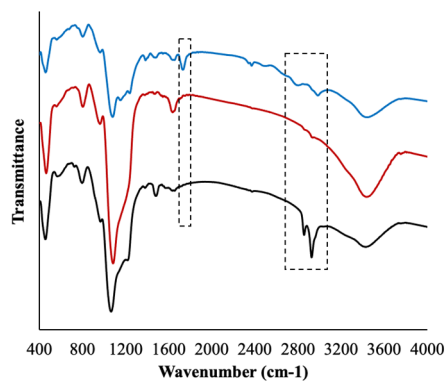


Figure 1. The Fourier-transform infrared (FT-IR) spectra of the nanoparticles: (black line) MSNs with the template, (red line) CTAB free initiated MSNs, (blue line) MSNs–PDEAEMA.

Nanoparticle morphology (size and shape) was studied using scanning electron microscopy (SEM) and transmission electron microscopy (TEM). Figure 2A shows the SEM images of the as-made MSNs particles with a particle size ranging from 250 nm up to approximately 350 nm with an almost spherical shape. The MSNs-PDEAEMA nanoparticles have a larger average particle size, ranging from 270 to 360 nm, as illustrated in Figure 2B.

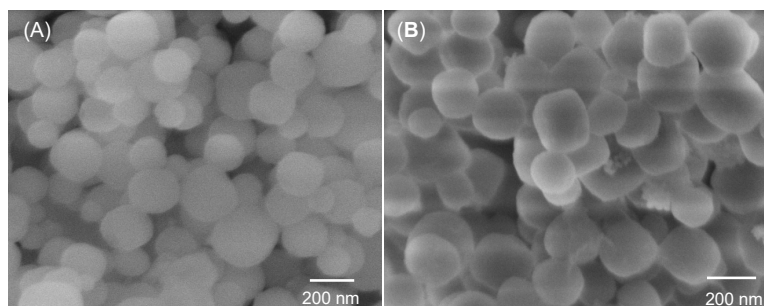


Figure 2. The morphology and mesostructure of nanoparticles: (A) SEM image of MSNs and (B) SEM image of PDEAEMA-MSNs.

The TEM technique was also used to examine the morphology and pore structure of the MSNs and MSNs-PDEAEMA. TEM images for MSNs showed almost spherical particles, having a size ranging from 250 nm to 350 nm and a clear pore structure with pore size of ca. 5 nm (Figure 3A). A thin organic layer (shell) could be seen on the outer surface of MSNs-PDEAEMA (Figure 3B). The dry thickness of polymeric shell was estimated to be ca. 20 nm.

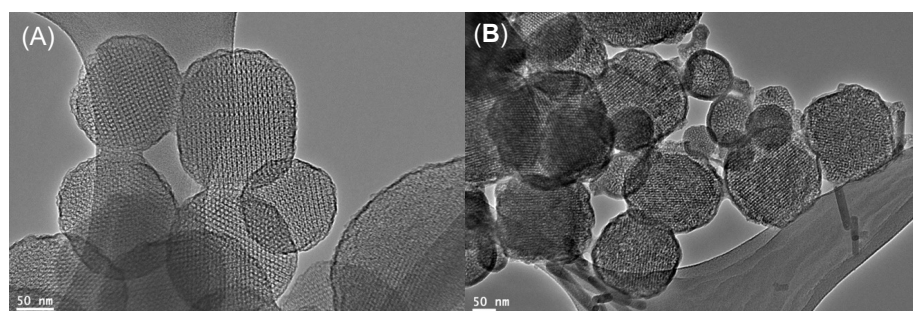


Figure 3. The morphology and mesostructure of nanoparticles: (A) TEM image of MSNs, and (B) TEM image of PDEAEMA-MSNs.

Narrow-scan x-ray photoelectron spectroscopy (XPS) spectra of MSNs-PDEAEMA, MSNs-PDEAEMA-SH, and MSNs-PDEAEMA-POEGMEA was used to confirm the successful modification of the surface of the polymer brushes with POEGMEA, as illustrated in Figure 4. XPS spectrum of C1s peak for MSNs-PDEAEMA was fitted with three components at binding energy 284.8, 286.1, and 288.0 eV, appointed to C-H, C-N/C-O, and O=C-O, respectively (Figure 4A). The peaks corresponding to C-N and C-O were overlapped; hence they were fitted using a single component. The calculated peak area ratios of the polymer composition were found to be in reasonable agreement with theoretical peak area ratios. No noticeable changes were observed in the deconvoluted peak after MSNs-PDEAEMA-SH, as shown in Figure 4B. After POEGMEA attachment, the C1s spectra was fitted with four peaks, corresponding to C-H, C-N, C-O, and O=C-O at binding energy of 284.9, 285.8, 286.3, and 288.6 eV, respectively. It was observed that the peak intensity of C-O increased as a result of the presence of additional C-O bonds contributed by the POEGMEA molecules (which confers seven polymerized ethylene glycol units per molecule), as shown in Figure 4C.

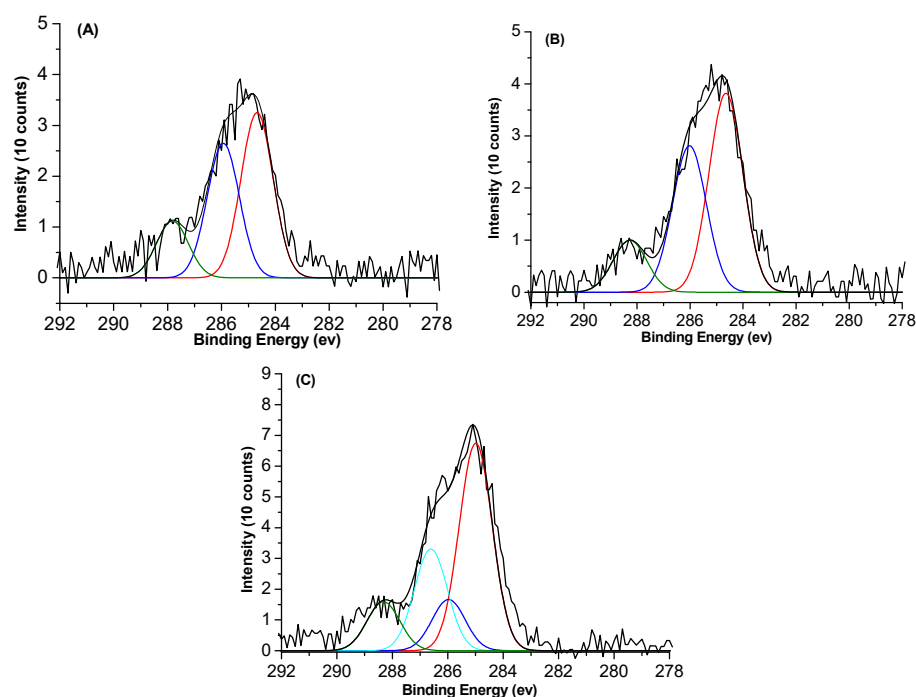


Figure 4. X-ray photoelectron (XPS) high-resolution C1s spectra of (A) MSNs-PDEAEMA, (B) MSNs-PDEAEMA-SH, and (C) MSNs-PDEAEMA-POEGMEA.

The pH-responsive behavior of MSNs-PDEAEMA, MSNs-PDEAEMA-SH, and MSNs-PDEAEMA-POEGMEA were also explored at 25 °C. As illustrated in Figure 5A, the size distribution of MSNs-PDEAEMA and the average hydrodynamic diameter (D_h) were determined at different pH using dynamic light scattering (DLS). At pH < 7, the D_h of the sample was ca. 300–1000 nm. The hydration layer had a larger particle diameter distribution due to the repulsion force between the polymer chains. When the brushes became hydrophobic in basic media, the hydrodynamic diameter of sample was found to be between 200 and 400 nm.

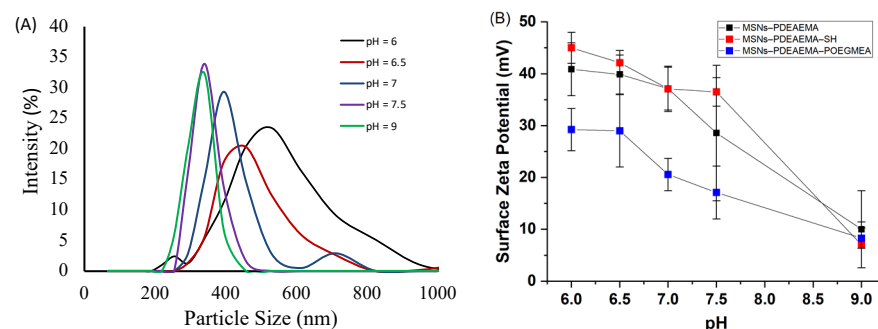


Figure 5. (A) Size distribution at different pH values of MSNs-PDEAEMA. (B) Zeta potential values at different pH and 25 °C for MSNs-PDEAEMA, MSNs-PDEAEMA-SH, and MSNs-PDEAEMA-POEGMEA.

When MSNs-PDEAEMA, MSNs-PDEAEMA-SH, and MSNs-PDEAEMA-POEGMEA became fully protonated in acidic media, the zeta potential was positively charged, whereas the zeta potential became close to zero when the brushes were deprotonated, as shown in Figure 5B. However, the zeta potential of MSNs-PDEAEMA-POEGMEA exhibited a lower value in acidic media with ca. 30 mV, compared to 42 mV for MSNs-PDEAEMA and MSNs-PDEAEMA-SH. At pH 9, the zeta potential of all examined nanosystems was ca. 8 mV, due to the deprotonation process of tertiary amines present in the polymer chains.

The RhB dye-loading capacity in the synthesized nanomaterials (MSNs-PDEAEMA, MSNs-PDEAEMA-SH, and MSNs-PDEAEMA-POEGMEA) was determined using Equation (1).

The loading capacity was found to be similar, ca. 74%, for all selected samples. FTIR technique was used to confirm the successful RhB dye-loaded into the system. Two peaks were observed at ~ 1400 and ~ 1570 cm^{-1} , pointed to C–C stretches of the aromatic ring in the dye's molecule (data not shown).

The released amount of the RhB dye was examined from the selected samples in buffer solutions at different pH values (5, 6.5, 7.4, and 8). For CTAB free MSNs, the dye release was noticed to be the same at different pH values. The dye release behavior was found to be similar for the three-polymer shell coated MSNs, in both basic and acidic media, as shown in Figure 6. The cumulative dye released from all examined samples reached 60% after ca. 8 h, when the nanosystems were exposed to a solution of pH 5 and 6.5. Such fast dye release could be referred to the protonation process of the tertiary amine presented in PDEAEMA segments. However, in basic media, almost 22% of the loaded dye was released within ca. 12 h from both MSNs–PDEAEMA and MSNs–PDEAEMA–SH, as presented in Figure 6A,B. A notable difference was observed in the release profile of the dye loaded in MSNs–PDEAEMA–POEGMEA in basic media. The dye was released from MSNs–PDEAEMA–POEGMEA with an accelerated drug release of ca. 15% after 15 h (Figure 6C). These results indicated that POEGMEA molecules capped with MSNs–PDEAEMA could hinder the dye release.

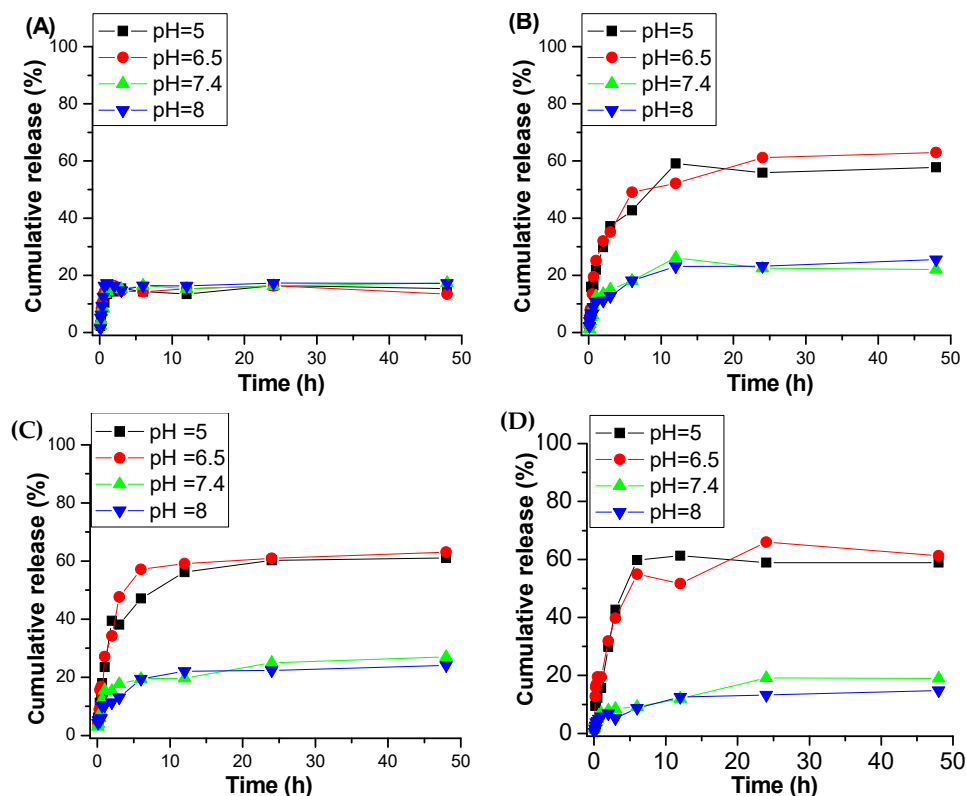


Figure 6. Dye release profiles of RhB loaded in (A) CTAB free MSNs, (B) MSNs–PDEAEMA, (C) MSNs–PDEAEMA–SH, and (D) MSNs–PDEAEMA–POEGMEA, at different pH and 37 °C.

Cytotoxicity assay showed that all three fabricated nanoparticles (MSNs–PDEAEMA, MSNs–PDEAEMA–SH, and MSNs–PDEAEMA–POEGMEA) were non-toxic to the hMSCs, as shown in Figure 7. The cytotoxicity assay of MSNs–PDEAEMA at all three concentrations were statistically the same, even after 48 h of incubation; however, there is some slight increase in cell proliferation, but it is statistically insignificant. MSNs–PDEAEMA–SH was not toxic to cells, although there was some statistically significant increase in cell proliferation for the 50 $\mu\text{g}/\text{mL}$ after 24 h of incubation. After 48 h, both 50 and 100 $\mu\text{g}/\text{mL}$ showed a substantial increase in cell proliferation but with no toxicity. MSNs–PDEAEMA–POEGMEA was non-toxic at all three concentrations after both 24 and 48 h of incubation.

However, after 48 h there was an increase in cell proliferation. All these positive results certify that the designed fabricated nanosystem exhibits an excellent biocompatibility that has the potential to be utilized as carriers for anti-cancer drugs delivery.

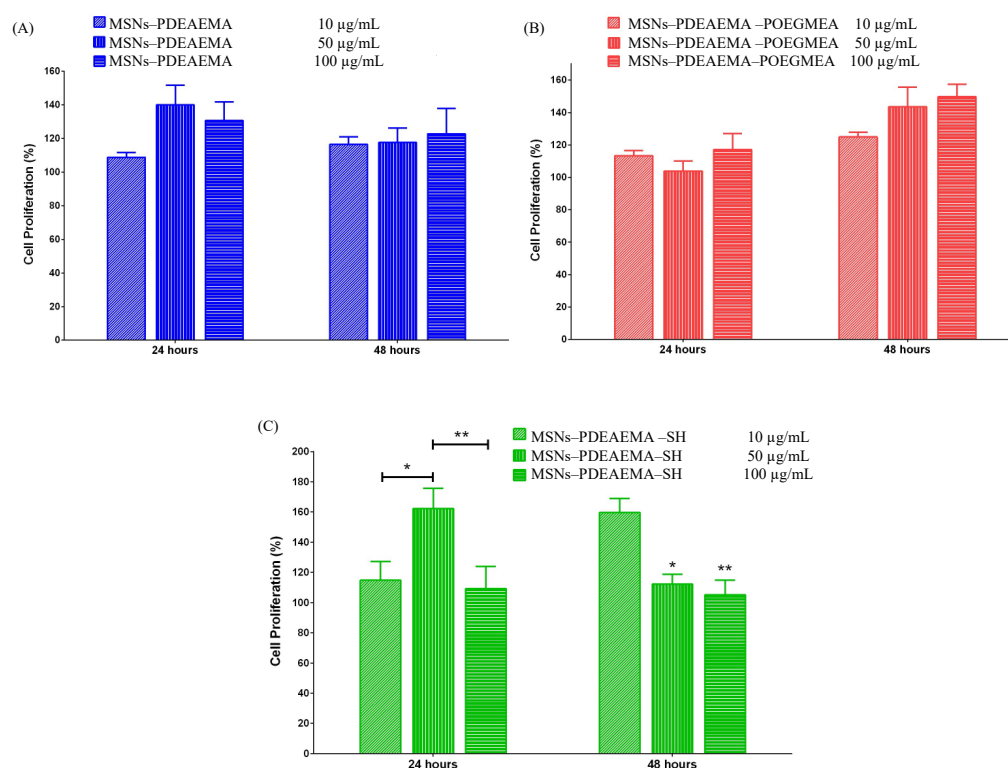


Figure 7. Cell viability of human bone marrow-derived mesenchymal stem cells (hMSCs) after exposure to the selected nanosystems. Cells were exposed for 24 h and 48 h to 10, 50, and 100 µg/mL of: (A) MSNs-PDEAEMA, (B) MSNs-PDEAEMA-POEGMEA, and (C) MSNs-PDEAEMA-SH. Astride indicate the level of significance as follows: * $P > 0.05$, ** $P > 0.01$.

4. Conclusions

In this paper, pH-responsive brush-modified particles have been obtained by growing PDEAEMA brushes on ca. 250 nm MSNs via surface-initiated ATRP technique. Halogens at the end of polymer chains were successfully derivatized to primary amines, which has elaborated strategies that allow modification of these brushes with molecules. POEGMEA have reacted successfully with thiol via thiol-Michael addition. XPS confirmed the successful attachment of POEGMEA molecules when the peak intensity of C–O increased, resulting from the presence of additional C–O bonds in the POEGMEA. The encapsulation efficiency of Rh B was found to be ca. 74% for all selected samples. The dye release profiles illustrated that the high release rate (ca. 60%) occurred when brushes are protonated at low pH, compared to the release rate in basic media (ca. 20%). MSNs-PDEAEMA, MSNs-PDEAEMA-SH, and MSNs-PDEAEMA-POEGMEA were found to be non-toxic to hMSC. Nevertheless, the results showed an increase in cell proliferation in some instances, without being statistically significant, except in the case of MSNs-PDEAEMA-POEGMEA at 50 µg/mL after both 24 and 48 h of incubation. This finding may indicate a potential role where cell proliferation is desirable, as in wound healing cases.

Author Contributions: Data curation, A.A. (Amal Alfawaz), A.B., and R.L.; formal analysis, K.A. (Khalid Alzahrani), A.N., H.A., L.A., and A.A. (Abdullah Alswieleh); writing—original draft preparation, K.A. (Khalid Alotaibi) and A.A. (Abdullah Alswieleh). All authors have read and agreed to the published version of the manuscript.

Funding: This research received no external funding.

Data Availability Statement: The data presented in this study are included in this article.

Acknowledgments: The authors extend their appreciation to the Deanship of Scientific Research at King Saud University for funding this work through research group no. RG-1439-026.

Conflicts of Interest: The authors declare that they have no conflict of interest.

References

1. Bray, F.; Ferlay, J.; Soerjomataram, I.; Siegel, R.L.; Torre, L.A.; Jemal, A. Global cancer statistics 2018: GLOBOCAN estimates of incidence and mortality worldwide for 36 cancers in 185 countries. *CA A Cancer J. Clin.* **2018**, *68*, 394–424. [[CrossRef](#)] [[PubMed](#)]
2. Li, Q.; Sun, A.; Si, Y.; Chen, M.; Wu, L. One-pot synthesis of polysaccharide–diphenylalanine ensemble with gold nanoparticles and dye for highly efficient detection of glutathione. *Chem. Mater.* **2017**, *29*, 6758–6765. [[CrossRef](#)]
3. Shao, P.; Wang, B.; Wang, Y.; Li, J.; Zhang, Y. The application of thermosensitive nanocarriers in controlled drug delivery. *J. Nanomater.* **2011**, *2011*, 1–12. [[CrossRef](#)]
4. Khan, R.U.; Yu, H.; Wang, L.; Zhang, Q.; Xiong, W.; Nazir, A.; Fahad, S.; Chen, X.; Elsharaarani, T. Synthesis of polyorganophosphazenes and preparation of their polymersomes for reductive/acidic dual-responsive anticancer drugs release. *J. Mater. Sci.* **2020**, *55*, 8264–8284. [[CrossRef](#)]
5. Bae, Y.H.; Park, K. Advanced drug delivery 2020 and beyond: Perspectives on the future. *Adv. Drug Deliv. Rev.* **2020**, *158*, 4–16. [[CrossRef](#)]
6. He, B.; Sui, X.; Yu, B.; Wang, S.; Shen, Y.; Cong, H. Recent advances in drug delivery systems for enhancing drug penetration into tumors. *Drug Deliv.* **2020**, *27*, 1474–1490. [[CrossRef](#)]
7. Barua, M.; Barua, S.; Mitragotri, S. Challenges associated with penetration of nanoparticles across cell and tissue barriers: A review of current status and future prospects. *Nano Today* **2014**, *9*, 223–243. [[CrossRef](#)]
8. Sanadgol, N.; Wackerlig, J. Developments of Smart Drug-Delivery Systems Based on Magnetic Molecularly Imprinted Polymers for Targeted Cancer Therapy: A Short Review. *Pharmaceutics* **2020**, *12*, 831. [[CrossRef](#)]
9. Carvalho, G.C.; Sábio, R.M.; de Cássia Ribeiro, T.; Monteiro, A.S.; Pereira, D.V.; Ribeiro, S.J.L.; Chorilli, M. Highlights in Mesoporous Silica Nanoparticles as a Multifunctional Controlled Drug Delivery Nanopatform for Infectious Diseases Treatment. *Pharm. Res.* **2020**, *37*, 191. [[CrossRef](#)]
10. Dilley, R.J.; Morrison, W.A. Vascularisation to improve translational potential of tissue engineering systems for cardiac repair. *Int. J. Biochem. Cell Biol.* **2014**, *56*, 38–46. [[CrossRef](#)]
11. Giri, S.; Trewyn, B.G.; Lin, V.S. Mesoporous silica nanomaterial-based biotechnological and biomedical delivery systems. *Na-nomedicine* **2007**, *2*. [[CrossRef](#)] [[PubMed](#)]
12. Descalzo, A.B.; Martínez-Mañez, R.; Sancenon, F.; Hoffmann, K.; Rurack, K. The supramolecular chemistry of organic–inorganic hybrid materials. *Angew. Chem. Int. Ed.* **2006**, *45*, 5924–5948. [[CrossRef](#)] [[PubMed](#)]
13. Silveira, C.P.; Apolinario, L.M.; Favaro, W.J.; Paula, A.J.; Duran, N. Doxorubicin-functionalized silica nanoparticles incorporated into a thermoreversible hydrogel and intraperitoneally administered result in high prostate antitumor activity and reduced cardiotoxicity of doxorubicin. *ACS Biomater. Sci. Eng.* **2016**, *2*, 1190–1199. [[CrossRef](#)] [[PubMed](#)]
14. Wang, X.; Li, X.; Ito, A.; Yoshiyuki, K.; Sogo, Y.; Watanabe, Y.; Yamazaki, A.; Ohno, T.; Tsuji, N.M. Hollow structure improved anti-cancer immunity of mesoporous silica nanospheres in vivo. *Small* **2016**, *12*, 3510–3515. [[CrossRef](#)]
15. Song, N.; Yang, Y.-W. Molecular and supramolecular switches on mesoporous silica nanoparticles. *Chem. Soc. Rev.* **2015**, *44*, 3474–3504. [[CrossRef](#)]
16. Keshavarz, H.; Khavandi, A.; Alamolhoda, S.; Naimi-Jamal, M.R. pH-Sensitive magnetite mesoporous silica nanocomposites for controlled drug delivery and hyperthermia. *RSC Adv.* **2020**, *10*, 39008–39016. [[CrossRef](#)]
17. Pande, A.M.; Andronescu, C.; Ghebaur, A.; Garea, S.A.; Iovu, H. New biocompatible mesoporous silica/polysaccharide hybrid materials as possible drug delivery systems. *Materials* **2019**, *12*, 15. [[CrossRef](#)]
18. Yousefpour, P.; McDaniel, J.R.; Prasad, V.; Ahn, L.; Li, X.; Subrahmanyam, R.; Weitzhandler, I.; Suter, S.; Chilkoti, A. Genetically encoded albumin binding into chemotherapeutic-loaded polypeptide nanoparticles enhances their antitumor efficacy. *Nano Lett.* **2018**, *18*, 7784–7793. [[CrossRef](#)]
19. Beagan, A.M.; Alghamdi, A.A.; Lahmadi, S.S.; Halwani, M.A.; Almeataq, M.S.; Alhazaa, A.N.; Alotaibi, K.M.; Alswieleh, A.M. Folic acid-terminated poly (2-diethyl amino ethyl methacrylate) brush-gated magnetic mesoporous nanoparticles as a smart drug delivery system. *Polymers* **2021**, *13*, 59. [[CrossRef](#)]
20. Manzano, M.; Vallet-Regí, M. New developments in ordered mesoporous materials for drug delivery. *J. Mater. Chem.* **2010**, *20*, 5593–5604. [[CrossRef](#)]
21. Wilczewska, A.Z.; Niemirowicz, K.; Markiewicz, K.H.; Car, H. Nanoparticles as drug delivery systems. *Pharmacol. Rep.* **2012**, *64*, 1020–1037. [[CrossRef](#)]
22. Tang, F.; Li, L.; Chen, D. Mesoporous silica nanoparticles: Synthesis, biocompatibility and drug delivery. *Adv. Mater.* **2012**, *24*, 1504–1534. [[CrossRef](#)] [[PubMed](#)]
23. Han, J.; Zhao, D.; Li, D.; Wang, X.; Jin, Z.; Zhao, K. Polymer-based nanomaterials and applications for vaccines and drugs. *Polymers* **2018**, *10*, 31. [[CrossRef](#)] [[PubMed](#)]

24. Chen, M.; Hu, J.; Wang, L.; Li, Y.; Zhu, C.; Chen, C.; Shi, M.; Ju, Z.; Cao, X.; Zhang, Z. Targeted and redox-responsive drug delivery systems based on carbonic anhydrase IX-decorated mesoporous silica nanoparticles for cancer therapy. *Sci. Rep.* **2020**, *10*, 14447. [[CrossRef](#)]
25. Mura, S.; Nicolas, J.; Couvreur, P. Stimuli-responsive nanocarriers for drug delivery. *Nat. Mater.* **2013**, *12*, 991–1003. [[CrossRef](#)]
26. Khorsand, B.; Lapointe, G.; Brett, C.; Oh, J.K. Intracellular drug delivery nanocarriers of glutathione-responsive degradable block copolymers having pendant disulfide linkages. *Biomacromolecules* **2013**, *14*, 2103–2111. [[CrossRef](#)]
27. Vaupel, P.; Kallinowski, F.; Okunieff, P. Blood flow, oxygen and nutrient supply, and metabolic microenvironment of human tumors: A review. *Cancer Res.* **1989**, *49*, 6449–6465.
28. Alswieleh, A.M.; Alshahrani, M.M.; Alzahrani, K.E.; Alghamdi, H.S.; Niazy, A.A.; Alsilme, A.S.; Beagan, A.M.; Alsheheri, B.M.; Alghamdi, A.A.; Almeataq, M.S. Surface modification of pH-responsive poly (2-(tert-butylamino) ethyl methacrylate) brushes grafted on mesoporous silica nanoparticles. *Des. Monomers Polym.* **2019**, *22*, 226–235. [[CrossRef](#)]
29. Cheesman, B.T.; Willott, J.D.; Webber, G.B.; Edmondson, S.; Wanless, E.J. pH-responsive brush-modified silica hybrids synthesized by surface-initiated ARGET ATRP. *ACS Macro Lett.* **2012**, *1*, 1161–1165. [[CrossRef](#)]
30. Beagan, A.; Lahmadi, S.; Alghamdi, A.; Halwani, M.; Almeataq, M.; Alhazaa, A.; Alotaibi, K.; Alswieleh, A. Glucosamine Modified the Surface of pH-Responsive Poly (2-(diethylamino) ethyl Methacrylate) Brushes Grafted on Hollow Mesoporous Silica Nanoparticles as Smart Nanocarrier. *Polymers* **2020**, *12*, 2749. [[CrossRef](#)]
31. Suk, J.S.; Xu, Q.; Kim, N.; Hanes, J.; Ensign, L.M. PEGylation as a strategy for improving nanoparticle-based drug and gene delivery. *Adv. Drug Deliv. Rev.* **2016**, *99*, 28–51. [[CrossRef](#)] [[PubMed](#)]
32. Mishra, P.; Nayak, B.; Dey, R. PEGylation in anti-cancer therapy: An overview. *Asian J. Pharm. Sci.* **2016**, *11*, 337–348. [[CrossRef](#)]
33. Kang, N.; Perron, M.-È.; Prud'Homme, R.E.; Zhang, Y.; Gaucher, G.; Leroux, J.-C. Stereocomplex block copolymer micelles: Core–shell nanostructures with enhanced stability. *Nano Lett.* **2005**, *5*, 315–319. [[CrossRef](#)]
34. Nik, A.B.; Zare, H.; Razavi, S.; Mohammadi, H.; Ahmadi, P.T.; Yazdani, N.; Bayandori, M.; Rabiee, N.; Mobarakeh, J.I. Smart drug delivery: Capping strategies for mesoporous silica nanoparticles. *Microporous Mesoporous Mater.* **2020**, *299*, 110115.
35. Alswieleh, A.M.; Beagan, A.M.; Alsheheri, B.M.; Alotaibi, K.M.; Alharthi, M.D.; Almeataq, M.S. Hybrid mesoporous silica nanoparticles grafted with 2-(tert-butylamino) ethyl methacrylate-b-poly (ethylene glycol) methyl ether methacrylate diblock brushes as drug nanocarrier. *Molecules* **2020**, *25*, 195. [[CrossRef](#)] [[PubMed](#)]
36. Alotaibi, K.M.; Almethen, A.A.; Beagan, A.M.; Alfahid, L.H.; Ahamed, M.; El-Toni, A.M.; Alswieleh, A.M. Poly (oligo (ethylene glycol) methyl ether methacrylate) Capped pH-Responsive Poly (2-(diethylamino) ethyl methacrylate) Brushes Grafted on Mesoporous Silica Nanoparticles as Nanocarrier. *Polymers* **2021**, *13*, 823. [[CrossRef](#)]
37. Feng, J.; Wen, W.; Jia, Y.-G.; Liu, S.; Guo, J. pH-responsive micelles assembled by three-armed degradable block copolymers with a cholic acid core for drug controlled-release. *Polymers* **2019**, *11*, 511. [[CrossRef](#)]